Coastal Dynamics 2017
Paper No. 093

DEPTH-INDUCED WAVE BREAKING CRITERIA IN DEPENDENCE ON WAVE NONLINEARITY IN COASTAL ZONE

Sergey Kuznetsov[1], Yana Saprykina[1]

Abstract

On the base of data of laboratory and field experiments, the regularities in changes in the relative limit height of breaking waves (the breaking index) from peculiarities of nonlinear wave transformations and type of wave breaking were investigated. It is shown that the value of the breaking index depends on the relative part of the wave energy in the frequency range of the second nonlinear harmonic. For spilling breaking waves this part is more than 35% and the breaking index can be taken as a constant equal to 0.6. For plunging breaking waves this part of the energy is less than 35% and the breaking index increases with increasing energy in the frequency range of the second harmonic. It is revealed that the breaking index depends on the phase shift between the first and second nonlinear harmonic (biphase). The empirical dependences of the breaking index on the parameters of nonlinear transformation of waves are proposed.

Key words: wave breaking, spilling, plunging, limit height of breaking wave, breaking index, nonlinear wave transformation

1. Introduction

Wave breaking is the most visible process of wave transformation when the waves approaching to a coast. The main reason is decreasing of water depth and increasing of wave energy in decreasing water volume. During breaking a wave energy is realized in a surf zone influencing on a sediments transport and on the changes of coastal line and bottom relief. The depth-induced wave breaking criteria which are used in modern numerical and engineering models are usually based on classical dependence between height of breaking wave (H) and depth of water (h) in breaking point:

$$H = \gamma h, \tag{1}$$

where γ – breaking index is adjustable constant and γ=0.8 is suitable for most wave breaking cases (Battjes, Janssen, 1978). The laboratory and field experimental data testify the wide range of γ (from 0.4 up to 1.2) and its dependence on bottom slope and wave steepness through Iribarren number (surf similarity parameter) (Battjes, 1974):

$$\mathrm{Ir} = \frac{\mathrm{tg}\alpha}{\sqrt{H/L}}, \tag{2}$$

where tg α is the inclination of the bottom, *H* is the characteristic height (e.g., the maximum or significant wave height at the breaking point), and *L* is the characteristic wavelength (in deep water or local, at the breaking point). As well, with an increase in the surf similarity parameter, the limit relative wave height on the whole also increases, but this dependence has a quite wide scatter and is observed only as a trend (Battjes, 1974). It has been noted that formula (1) best describes wave breaking over a gently sloping bottom and is hardly satisfied at all for waves propagating over a steep bottom. This may be related to the significant influence of reflection on the height of breaking waves (Chella, et al., 2015; Rattanapitikon, Vivattanasirisak, 2002).

[1]P.P.Shirshov Institute of Oceanology of Russian Academy of Sciences, Moscow, Russia, kuznetsov@ocean.ru, saprykina@ocean.ru

Dependence (1) is applied in many modern models for waves in the coastal zone to describe their energy dissipation during breaking (e.g., MIKE21, certain modifications of SWAN).
In nature, waves are irregular; therefore, in practice, it is convenient to use criteria based on relations (1), but written for the significant height of waves determined from the wave spectrum as

$$H_s = 4\sqrt{m_0} \quad (3)$$

where $m_0 = \int_0^\infty S(\omega)d\omega$, S is the wave spectrum, ω - frequency.

As a result of verifying different well-known empirical formulas for the breaking index when they use the height of significant waves, it has been established that its values on average will be on the order of 75% of the values obtained for the empirical formulas for the limit height of breaking single and regular waves (Kamphuis, 1991). Thus, in formula (1), instead of the height of single waves, we take the significant height of waves, then the value of the most frequently used breaking index with be on the order of 0.6. Similar estimates for breaking waves of the root mean square height (H_{rms}) were obtained in (Thornton, Guza, 1983):

$$H_{rms}=0.42h,$$

or, taking into account that $H_s = 1.41H_{rms}$,

$$H_s = 0.59h \quad (4)$$

The variability of the breaking index, in our opinion, is determined by the physical processes of nonlinear wave transformation above an inclined bottom, which manifest themselves differently depending on the bottom inclination and the initial wave steepness (e.g., Saprykina et al., 2013). This has been partially confirmed by the results of other researchers. For example, in (Salmon, Holthuijsen, 2015), in verifying formula (1) based on field data, it was noted that the size of the breaking index depends on shallow water conditions during wave transformation, which are determined by the parameter *kh (*wave number *k* and depth of water *h*) and the slope of the bottom. Account of these parameters in their proposed modified formula for the breaking index has made it possible to increase by 10--15% the accuracy of calculating of energy losses of breaking waves in the SWAN model. For this model, it was also noted that the introduction of a nonlinear correction in the form of a change in the phase shift (biphase) between multiple harmonics of wave motion into the formula for calculating wave energy dissipation significantly increases the accuracy in modeling breaking waves (Westhuysen, 2010). Unfortunately, these studies are limited to refining the mathematical formulas for describing wave energy dissipation; they do not study the features of the physical process of their transformation leading to breaking.
The variations of γ can be explained by the distinctions of the amplitude-phase frequency structure of waves before its breaking due to nonlinear wave transformation. According to some laboratory and numerical studies, the type of wave breaking can also influence the size of the breaking index (e.g., Chen, Li, 2015). Earlier, we showed that the type of breaking - plunging or spilling - depends on the wave asymmetry determined by the relation of the amplitudes of the first and second nonlinear harmonics and the phase shift between them (Kuznetsov et al., 2015).
The main purpose of this work is to explain how the depth induced breaking criteria (1) depends on the features of nonlinear wave transformation in coastal zone.

2. Experiments and methods

For an analysis the data of two experiments were used. A laboratory experiment on quasimonochromatic wave transformation above a uniform inclined bottom with a different inclination was performed in 2013 at the Sea Shores scientific research center in Sochi (for more details, see, e.g., Saprykina et al., 2015). Length of the flume is 22 m, width - 0.8 m, depth - 1 m. Waves were measured by 14 digital wire capacity-type gauges placed along the length of an underwater slope, synchronously with a sample rate of 25 Hz. Duration of each wave run was about 4 min. The type of wave breaking and the location of the wave breaking point were determined visually and recorded with photo and video equipment. In cases where wave breaking occurred between gauges, the relation between the height of a breaking wave and the water depth at the breaking point was calculated for the location of the gauge nearest to the breaking point.

A field experiment was performed in 2007 on an experimental pier at the Institute of Oceanology, Bulgarian Academy of Sciences, near the village of Shkorpilovtsy on the Black Sea (for more details, see, e.g., Saprykina et al., 2009; 2013). To record waves, 15 wire wave gauges were used: seven capacitive type gauges and eight resistance type gauges evenly placed along the length of the pier (250 m) at depth range 0.5 m - 4 m. Measurements at 15 points were conducted synchronously with a sampling rate from 5 to 20 Hz. The durations of wave records were from 20 min up to 1 hour. The bottom profile in the experimental area had a medium inclination of 0.024 and contained an underwater bar.

The location of wave breaking points and the type of breaking were recorded visually and photographically. Depending on the wave regime, from one to three breaking lines were observed. Just like in the laboratory experiment, as wave breaking occurred between gauges, the relation between the height of a breaking wave and the water depth at the breaking point was calculated for the location of the gauge nearest to the breaking point.

In addition to limit significant height of breaking waves (4) we considered steepness of breaking waves H_s/L_b, L_b - wavelength of breaking wave; it was calculated for the period of the spectral peak of irregular waves.

We also analyzed:

a) the coefficient of wave asymmetry with respect to the horizontal

$$Sk = \frac{\langle \zeta^3 \rangle}{\sigma^3}, \quad (5)$$

and vertical

$$As = \frac{\langle \zeta_H^3 \rangle}{\sigma^3} \quad (6)$$

axis, where $\langle\ \rangle$ is the averaging operator, ζ is the free surface elevations (wave chronograms), σ is the standard deviation of the free surface elevations, and ζ_H is Hilbert transform of a wave chronogram.

b) The ratio of the wave energy in the frequency range of the second nonlinear harmonic to the wave energy in the frequency range of the main harmonic, which corresponds to the frequency of the main spectral maximum. The boundary of splitting into frequency ranges was determined visually by the minimum of the spectral energy between the spectral maxima of the main and second harmonics. The lower boundary of the frequency range of the first harmonic was taken as 0.05 Hz, and the upper boundary of the frequency region of the second harmonic, 1.5 from the frequency of the second harmonic.

c) The phase shift between the first and second nonlinear harmonics are calculated by the following formula (Kim, Powers, 1979):

$$\beta(\omega_1, \omega_2) = \arctan\left[\frac{\mathrm{Im}\{B(\omega_1,\omega_2)\}}{\mathrm{Re}\{B(\omega_1,\omega_2)\}}\right], \quad (7)$$

where $B(\omega_1,\omega_2) = A_{\omega_1} A_{\omega_2} A^*_{\omega_1+\omega_2}$ is the bispectrum, ω is the angular frequency, and *A* are the complex Fourier amplitudes of the chronogram of free surface elevations. The frequencies of the first and second harmonics were determined by the positions of the local maxima of the wave spectrum.

3. Discussion of results

According to criteria (1) waves break when their height becomes larger than the critical values. Figure 1 shows the limit height of breaking waves as a function of their steepness.

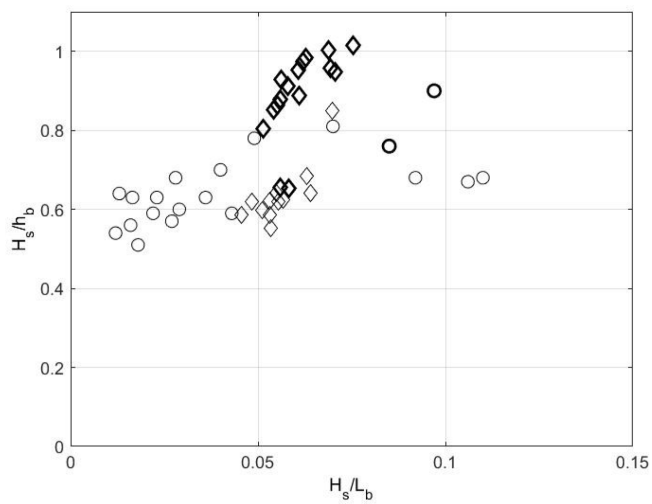

Figure 1. Dependence of breaking index on wave steepness at breaking point. Circles - laboratory experiment; diamonds- experiment. Bold symbols correspond to waves breaking as plunging type; plain symbols, waves breaking as spilling type.

On the whole, it is possible to say that the steeper the wave, the larger the breaking index (Fig. 1). However, in a detailed consideration, it is impossible to establish an unambiguous relationship between the wave steepness parameter and the breaking index or the relative wave height at the breaking point. For example, waves having the same steepness in the range of $0.05 < H/L < 0.065$ can have difference breaking indexes: close to the mean (on the order of 0.6) and substantially higher that the mean. Meanwhile, for the same wave steepness, these waves have a different type of breaking. Laboratory modeling shows that an increase in wave steepness to values larger than 0.08 does not lead to increase in the breaking index. Thus, breaking waves do not have an unambiguous relationship between their steepness and the limit height, whereas the wave steepness is not a sufficient parameter to characterize the limit height of breaking waves.

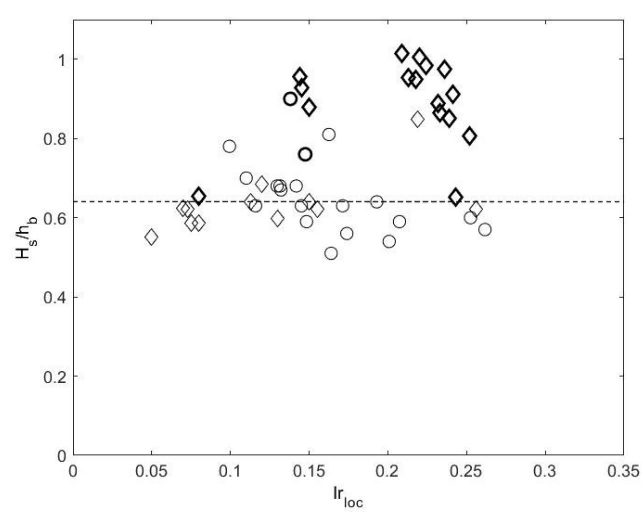

Figure 2. Dependence of breaking index on parameter of similarity to coastal zone (Iribarren number) at breaking point. Circles - laboratory experiment; diamonds- experiment. Bold symbols correspond to waves breaking as plunging type; plain symbols, waves breaking as spilling type.

The trend described in (Battjes, 1974) of an increase in the breaking index of individual waves with an increase in the Iribarren number for the breaking index of the heights of significant waves is not as obvious (Fig. 2). It is possible to state that two trends are observed simultaneously. The first is when the breaking index on average depends weakly on the Iribarren number, which is characteristic of waves breaking predominantly by spilling, and its deviations from 0.6 are no more than 15%. The deviations observed in the data may be related to an error in the positioning of the breaking point. When breaking occurred between to sequential wave-recording gauges, the breaking index was calculated by the data of the gauge nearest to the breaking point.

The second trend is when the breaking index increases with an increasing Iribarren number. Here, large breaking indexes correspond to waves breaking predominantly by plunging. An increase in the breaking index values may not be related to the influence of the bottom inclination on wave transformation to a large degree, because the data of numerical modeling performed over different bottom inclinations show no significant differences in their values with increasing Iribarren number. Conversely, all of its values for the modeling data vary around 0.6.

Increased breaking index values (greater that 0.8) may not be unambiguously related to waves reflected from the slope, because, as shown in (Saprykina et al., 2015), the coefficient of local wave reflection from shore has large values at distances on the order of the wavelength and significantly decreases at large distances.

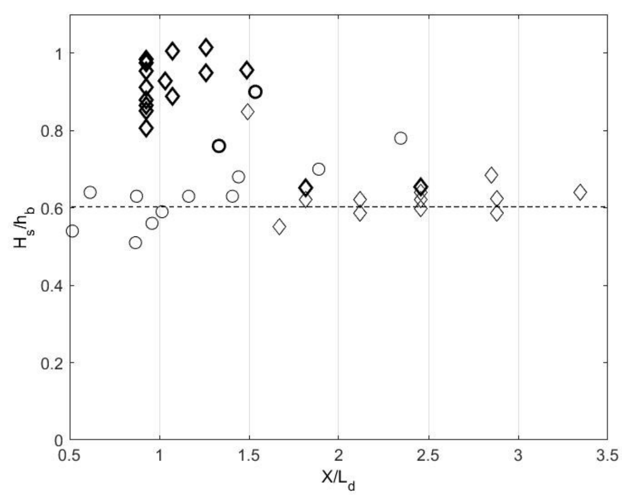

Figure 3. Dependence of breaking index on relative distance to shore at breaking point. Circles - laboratory experiment; diamonds- experiment. Bold symbols correspond to waves breaking as plunging type; plain symbols, waves breaking as spilling type.

As seen in Fig. 3, large breaking indexes are observed for waves breaking at distances from shore on the order of the corresponding wavelength in deep water. Meanwhile, waves breaking closer to shore have a small breaking index.

The wave transformation conditions depend on the relative wave height *h/L*. Figure 4 shows the dependence of a change in the relative limit height of breaking waves on the relative water depth at the breaking point. One can see that two different trends exist: for $h/L < 0.08$, the breaking index increases with increasing relative depth, and for $h/L > 0.06$, it decreases. As well, for relative depths $0.1 < h/L < 0.06$, the widest scatter of breaking index values is observed. The discussed relative depths for the considered breaking waves correspond to the conditions of the weakly nonlinear-dispersive wave transformation, a characteristic peculiarity of which is near-resonance three-wave interactions, during which the amplitudes of the first and second nonlinear wave harmonics can exchange energy. As well, the amplitude of the second harmonic can reach values comparable to the amplitude of the first harmonic (Saprykina et al., 2009, 2013). During nonlinear interaction between the harmonics, not only their amplitudes vary, but also the phase shift (biphase) between them, which depends on the stages of energy exchange between the harmonics (Saprykina et al., 2017).

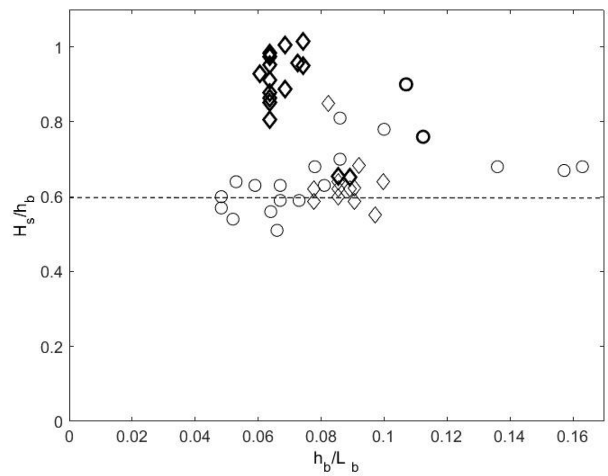

Figure 4. . Dependence of breaking index on relative water depth at breaking point. Circles - laboratory experiment; diamonds- experiment. Bold symbols correspond to waves breaking as plunging type; plain symbols, waves breaking as spilling type.

The simultaneous existence of two trends may be related to the different influence of the two main processes occurring with waves during their nonlinear transformation and causing waves to break: an increase in the second and higher nonlinear harmonics and changes in the phase shift between them and the main harmonic. For example, it is possible to assume that the instability of the waveform for relative depths $0.1 < h/L$ are more affected by phase shifts, and for $h/L < 0.06$, it is more affected by the values of the amplitude of the second harmonic. For $0.06 < h/L < 0.1$, both processes can have the same effect.
Figures 1-4 shows that the different observed trends for the breaking index values are also related to the predominant type of breaking. Increased breaking index values are characteristic of waves breaking by plunging, whereas for waves of the spilling type, the breaking index on average is 0.6. The type of wave breaking is determined by their spectral composition and depends on the stage of wave transformation and, in particular, on the evolution of the second nonlinear harmonic. Let us consider how the spectral composition of waves affects the limit height of breaking waves.

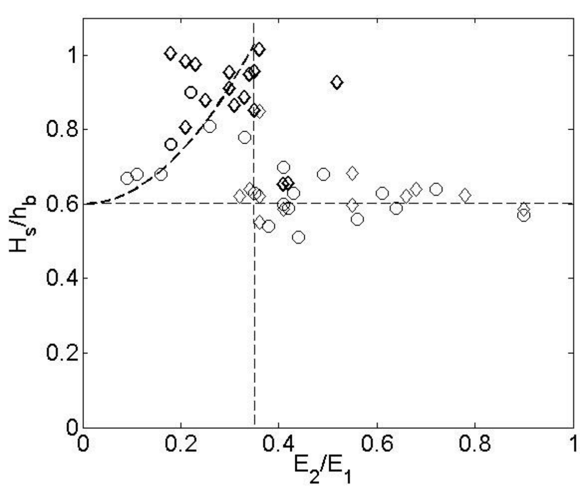

Figure 5. Dependence of breaking index on relative size of energy of second nonlinear harmonic at breaking point. Circles - laboratory experiment; diamonds- experiment. Bold symbols correspond to waves breaking as plunging type; plain symbols, waves breaking as spilling type.

Figure 5 shows the dependence of the breaking index on the size of the energy of the second harmonic, which is related to the size of the energy of the first harmonic.

In the experimental data, an increase in the limit relative height of breaking waves is characteristic of waves in which the amplitude of the second harmonic is approximately less that 35%. For these waves, the breaking index increases with increasing relative amplitude of the second harmonic, which can be approximated for the available data, e.g., by a quadratic dependence.

$$\gamma = H_s/h_b = 0.6 + 3.5(E_2/E_1)^2. \tag{8}$$

For waves having relative amplitude of the second harmonic more that 35%, the breaking index does not increase with its growth; they are characterized by an approximately uniform distribution of the breaking index with respect to its mean value of 0.6.

Note that small amplitudes of the second harmonic and an increase in the limit height of breaking waves with an increase in the amplitude of the second harmonic is characteristic of waves breaking predominantly by plunging. Large relative amplitudes of the second harmonic correspond to waves breaking by spilling. This completely corresponds to and once again confirms the conclusions drawn in (Kuznetsov et al., 2015).

The size of the maximum relative energy of the second harmonic for wave transformation above an inclined bottom can be predicted from the steepness of waves (by the ratio of the height to the wavelength) on seaward boundary of the coastal zone and is inversely proportional to it according to the empirical dependence obtained in (Saprykina et al., 2015).

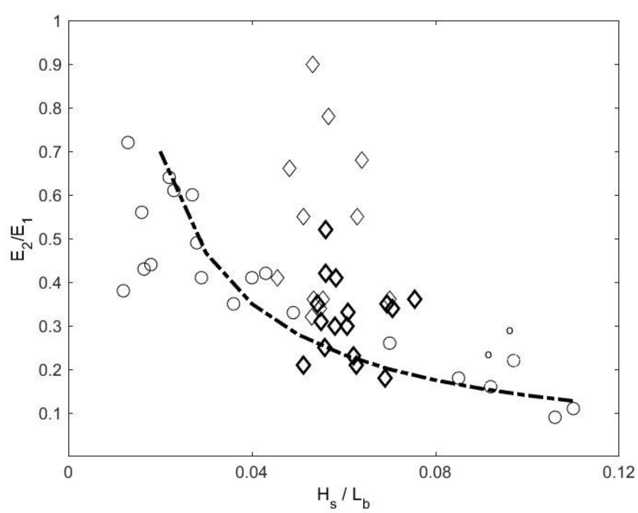

Figure 6. Dependence of relative energy of second harmonic on wave steepness at breaking point. Circles - laboratory experiment; diamonds- experiment. Bold symbols correspond to waves breaking as plunging type; plain symbols, waves breaking as spilling type.

Verification of this relation for the wave steepness at the breaking point according to the available data of field and laboratory experiments has shown that the dependence will have the same form (Fig.6):

$$E_2/E_1 = 0.014/(H_s/L_b), \tag{9}$$

where H_s is the height of significant waves and L_b in the wavelength at the breaking point. The empirical dependence of the relative energy of the second nonlinear harmonic on the wave steepness (9) is suitable for determining the share of energy of the second harmonic for $E_2/E_1) < 0.35$ (Fig. 6).

Another way to account energy of second harmonic is on the base of Ursell number. According to the second-order approximation for a stationary Stokes wave describing weakly nonlinear dispersion waves, the ratio of the amplitudes of the second and first nonlinear harmonics depends on the Ursell number for

$kh \to 0$: $$\frac{a_2}{a_1} \approx \frac{3}{4}\frac{ak}{(kh)^3} = \frac{3}{4}\mathrm{Ur}, \tag{10}$$

where k is the wavenumber; a_1, a_2 are the amplitudes of the first and second harmonics; h is depth; $a = H/2$, where H is the wave height (Dingemans, 1997). The ratio of the energy of the nonlinear harmonics, which is equal to the ratio of the amplitudes squared, will depend quadratically on the steepness and on the Ursell number, respectively.

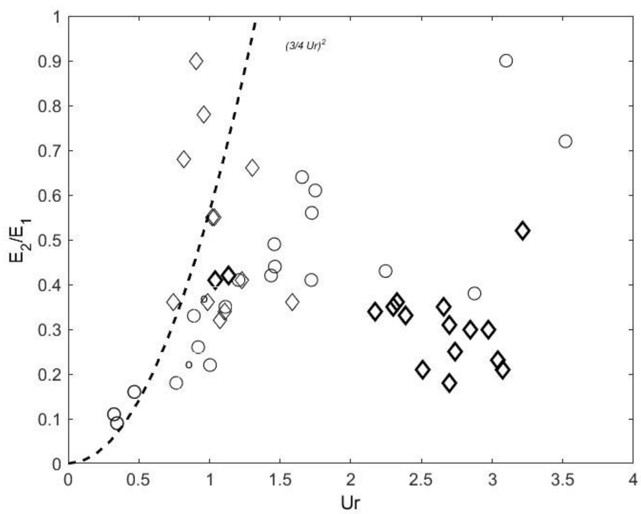

Figure 7. Dependence of relative energy of second harmonic on Ursell number. Circles - laboratory experiment; diamonds- experiment. Bold symbols correspond to waves breaking as plunging type; plain symbols, waves breaking as spilling type.

Figure 7 shows the dependence of the relative energy of the second nonlinear harmonic E_2/E_1 on the Ursell number. Clearly, for small Ursell numbers (Ur < 1), the relative energy of the second nonlinear harmonic in the experimental data corresponds well to weakly nonlinear dispersive Stokes waves and can be determined by formula (10). These waves break predominantly by spilling.
With an increase in the Ursell number and, accordingly, an increase in the influence of nonlinearity, the relative share of energy of the second harmonic is not described by relation (10). Such waves break predominantly by plunging (Fig.7).
Thus, the limit height of a breaking wave can be determined by formula (8) if one knows the size of the relative amplitude of the second harmonic, which is calculated by the empirical relation for local wave steepness (9) of for small Ursell numbers by the relation from Stokes second-order wave theory (10).
A different type of breaking also depends on wave asymmetry against vertical axis (Kuznetsov et al., 2015) and asymmetry coefficient linear depends on β - the phase shift between the first and second nonlinear harmonics (biphase) (Saprykina et al., 2017):

$$As = 0.8\beta \tag{11}$$

Figure 8 shows the dependence of the breaking index on the biphase of breaking waves. The breaking index increases with decreasing of biphase in general. But two main tendencies can be observed. For waves breaking mainly spilling type (biphase more then $-\pi/3$) the breaking index changes slightly, and for example, its value can be accepted to the constant which isn't depending on the biphase. And for waves breaking mainly plunging type (biphase less then $-\pi/3$) the breaking index increases with decreasing of the biphase.

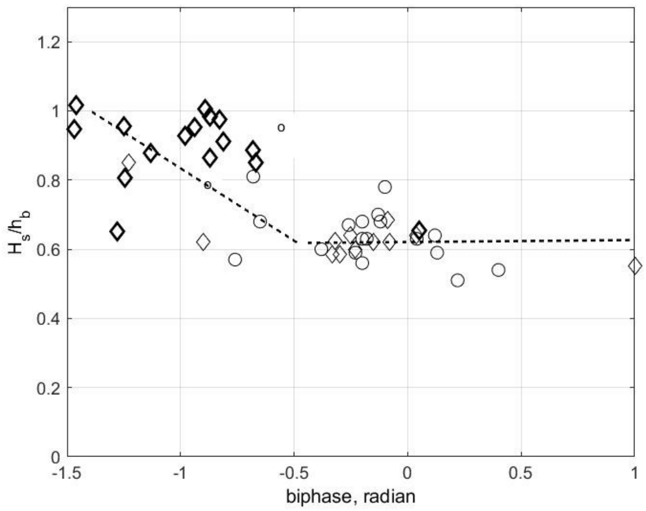

Figure 8. Dependence of breaking index on biphase at breaking point Circles - laboratory experiment; diamonds- experiment. Bold symbols correspond to waves breaking as plunging type; plain symbols, waves breaking as spilling type.

According to the available data, the dependence of the breaking index on the biphase for these waves is approximately linear:

$$\gamma = H_s/h_b = 0.6 - 0.24\ \beta, \qquad (12)$$

and $\gamma = H_s/h_b \approx 0.6$, if biphase is more then $-\pi/3$. This corresponds to waves breaking by spilling. So, if the biphase is known there is possible to define type of breaking and breaking index.
The empirical formula for determining the biphase from the bottom inclination, depth, and local wavenumber was proposed, e.g., in (Saprykina et al, 2017):

$$\beta = \pi/2\Delta l - \pi/2\ , \quad \text{for } \Delta l < 1, \qquad (13)$$

where $\Delta l = (h/\text{tg}\ \alpha)/L_b$, h is the local water depth, tg α is the local mean bottom inclination, and $L_b = 2\pi/(k_2 - 2k_1)$, $k_{1,2}$ are calculated from the dispersion relation of linear wave theory $\omega^2 = gk \tanh kh$.

4. Conclusions

As a result of analyzing the experimental data, it was established that nonlinear wave transformation influences the size of the breaking index, which determines the relation between the significant height of breaking irregular waves and the water depth at the breaking point. It depends on the relative share of the energy of the second nonlinear harmonic and the phase shift between the first and second nonlinear harmonics, which determines the wave asymmetry with respect to the vertical axis.
If the relative share of the energy of the second nonlinear harmonic is more than 35%, then the breaking index on average varies insignificantly and can be taken as equal to 0.6. As well, breaking waves will be asymmetric with respect to the horizontal axis and actually symmetric with respect to the vertical axis (the phase shift is close to zero), which corresponds to predominate breaking as the spilling type.
If the relative energy of the second nonlinear harmonic is less than 35%, then the breaking index is larger than 0.6 and will increase with an increase in the share of the energy in the frequency range of the second harmonic. As well, breaking waves will have a large asymmetry with respect to the vertical axis (the phase shift is negative and close to $-\pi/2$), but will be nearly symmetric with respect to the horizontal axis, which

corresponds to waves breaking predominantly by plunging.

It has been revealed that the asymmetry of breaking waves with respect to the vertical axis linearly depends on the phase shift between the first and second nonlinear harmonics.

It has been shown that in breaking waves, the ratio of the amplitudes of the second and first harmonics for Ursell numbers smaller than 1 is proportional to the Ursell number, which corresponds to Stokes' second-order wave theory.

Empirical dependences for calculating the breaking index using the share of energy of the second nonlinear harmonic and the biphase were proposed.

Acknowledgements

The study was supported by the Russian Science Foundation (grant no. 14-50-00095).

References

Battjes, J., J. P. F. M. Janssen, 1978. Energy loss and set-up due to breaking of random waves,*Proceedings of the 16th International Conf. on Coastal Engineering, Hamburg* : 569–587.

Battjes, J., 1974. Surf similarity, *Proceedings of the 14th International Conf. on Coastal Engineering, Copenhagen*: 466–480.

Chella, M. A., H. Bihs, M. Musculus, 2015. Breaking characteristics and geometric properties of spilling breakers over slope, *Coastal Eng.,* 95: 4–19.

Chen, Y.-Y., M.-S. Li., 2015. Evolution of breaking waves on sloping beaches, *Coastal Eng.* 95: 51–65.

Dingemans, M. W., 1997. Water wave propagation over uneven bottoms, in *Advanced Series on Ocean Engineering* , World Scientific, Singapore, Vol. 13: 171–184.

Kamphuis, J. W. 1991. Incipient wave breaking, *Coastal Eng.* , 15: 185–203.

Kim, Y., E. Powers, 1979. Digital bispectral analysis and its application to non-linear wave interaction, *IEEE Trans. Plasma Sci.*, 1: 120–131.

Kuznetsov, S. Yu., Ya. V. Saprykina, B. V. Divinskii, and M. N. Shtremel, 2015. Spectral structure of breaking waves, *Proceedings IMAM 2015 "Towards Green Marine Technology and Transport,* Taylor and Francis, London: 853-858.

Rattanapitikon, W., T. Vivattanasirisak, 2002. Comparison of breaker height formulas using large-scale wave tanks Songklanakarin, *J. Sci. Technol.*, 24 (4): 663–674.

Salmon J., L. Holthuijsen, 2015. Modeling depth-induced wave breaking over complex coastal bathymetries, *Coastal Eng*., 105: 21–35.

Saprykina, Ya. V., M. N. Shtremel, S. Y. Kuznetsov, 2017. About possibility of parametrization of evolution of biphase in coastal zone, *Oceanology,* 57: 76–88.

Saprykina, Ya. V., S. Y. Kuznetsov, A. N. Kovalenko, 2015. Experimental studies of the local reflection of long waves from an underwater slope, *Oceanology,* 55: 171–181.

Saprykina, Ya. V., S. Yu. Kuznetsov, M. N. Shtremel, V. Sundar, 2015. Evaluation of vulnerability of the coastal zone affected by waves on the example of the southern coast of the Indian subcontinent, *Processes in Geomedia*, No. 3, 76–88. (in Russian).

Saprykina, Ya. V., S. Yu. Kuznetsov, Zh. Cherneva, N. Andreeva, 2009. Spatio-temporal variability of the amplitude-phase structure of storm waves in the coastal zone of the sea, *Oceanology,* 49: 182–192.

Saprykina, Ya. V., S. Y. Kuznetsov, N. K. Andreeva, M. N. Shtremel, 2013. Scenarios of nonlinear wave transformation in the coastal zone, *Oceanology,* 53: 422-431.

Thornton, E., R. T. Guza, 1983. Transformation of wave height distribution, *J. Geophys. Res*. 88: 5925–5938.

Westhuysen, A. van der, 2010. Modeling of depth induced wave breaking under finite depth wave growth conditions*, J. Geophys. Res.* 115: C0108.